Chapter-2

Synthesis and Characterization Techniques

Chapter 2

Synthesis and Characterization Techniques

2.1 Overview

This chapter illustrates the methods adopted for fabrication, synthesizing, characterizing, and assessing electrode materials for high-performance energy storage devices. The fundamentals and operational characteristics of different characterization techniques like X-ray diffraction pattern (XRD), thermo-gravimetric analysis and differential scanning calorimetry (TGA– DSC), UV-visible absorption spectroscopy, fourier transform infrared spectroscopy (FT-IR), field emission scanning electron microscopy (FE-SEM) with energy dispersive X-ray analysis (EDAX or EDX), transmission electron microscopy (TEM) with high resolution micrograph analysis along with selected area electron diffraction (SAED) pattern studies, X-ray photoelectron spectroscopy (XPS), and electrochemical characterization with cyclic voltammetry (CV), electrochemical impedance spectroscopy (EIS), galvanostatic charge-discharge (GCD) were used to characterize the electrode material used in proposed studies.

2.2 Synthesis Technique

Nanomaterials have revolutionised various sectors, including electronics, health, and energy, owing to their extraordinary qualities and numerous uses. The synthesis of materials in the range of nano regime is the foremost step in nanotechnology research and development which may be divided into two categories: bottom-up and top-down. Bottom-up synthesis is creating nanomaterials from their atomic or molecular constituents. This method uses molecular recognition and self-assembly to produce materials with complex nanostructures. Bottom-up synthesis often uses chemical

vapour deposition, sol-gel, and hydrothermal techniques. Chemical synthesis methods have significant advantages during bottom-up synthesis. They can engineer materials at the atomic or molecular scale, allowing precise control over their composition, size, shape, and crystallinity. Top-down synthesis, in contrast to bottom-up synthesis, involves the fabrication of nanomaterials by the selective removal or modification of bulk materials. This method allows researchers to modify and mould materials by reducing their size from the macroscopic to the nanoscale. Sputtering, etching, and ball milling carve nanostructures from larger materials. Top-down and bottom-up synthesis processes have revolutionized the field of nanotechnology, offering exceptional control over the properties and opening up exciting pathways in areas such as energy storage, nanoelectronics, and biomedical applications. [1]

The choice of method depends on the specific application and the desired properties of the product. The material's morphology plays a vital role in deciding the suitability of the electrode material in energy storage applications. To conceive unique nanostructures, it is crucial to select the appropriate methodology. Researchers have developed different synthetic approaches to prepare TMSs. Solution-based procedures, such as coprecipitation [2, 3], electrodeposition [4, 5], hydro/solvothermal [6, 7], and self-template [8, 9] methods have often been employed more often than solid-state methods due to their facile process and controllability. Single-phase synthesis is essential to determine the properties of the material. There is no shape and size control in solid-state methods as they form thermodynamic stable products. In contrast, we can control the shape and size of development in solution-based methods and lead to the formation of single-phase materials as it is a kinetically controlled reaction. Primarily two synthesis routes were followed in this thesis.

2.2.1 Solid-State Method

The solid-state reaction approach is a well-established, reliable method for making materials directly from solid reagents, including inorganic compounds, organic compounds, and composite materials. High temperatures for a specified period are necessary to produce polycrystalline materials from the powder precursors using the technique above.

Chemical and morphological characteristics of the reagents, such as their reactivity, surface area, free energy change during the solid-state reaction, and other reaction parameters, including temperature, pressure, and the reaction environment, all influence the solid-state reaction. The simplicity of the method allows for large-scale production of various materials, which can be done without solvents. [10]

The flux method often called the flux synthesis method, is used for chemical synthesis in solid-state chemistry. This technique has been used to synthesize high-melting oxides, phosphate, arsenates, and ceramic crystals, which the usual solid-state approach cannot produce. The basic principle of the flux method is to dissolve the reactants in the flux material (typically a molten salt or a low melting point compound), which facilitates the formation of desired compounds at lower temperatures than would be required without the flux. The choice of flux material depends on the specific reaction and its ability to dissolve the reactants. Alkali metal halides, alkali metal hydroxide, alkaline earth metal halides, and transition metal halides are frequently used as flux materials. Lower reaction temperatures can help minimise undesired side reactions and improve the purity of the final product. Additionally, using a flux can enhance crystal growth and facilitate the formation of single crystals, which is essential in many fields of materials research. [11, 12]

2.2.2 Solution-Based Methods

Synthesis techniques and procedures involving the chemical reactions or synthesis of materials in a liquid media, usually a solvent, are referred to as solution-based synthesis methods. These methods are often cost-effective, low-temperature, environmentally friendly, and energy-efficient. [13] Some examples of methods used in solution-based synthesis are shown below:

Sol-gel method: This method is known as a sol-gel method because the liquid precursor is transformed into a sol during the synthesis of the nanoparticles, and the sol is ultimately converted into a network structure known as a gel. The gel is then treated to remove the solvent and subjected to other treatments like drying or calcination to achieve the required substance. Sol-gel method is used to produce thin films, glasses, ceramics, and nanoparticles.

Hydro/Solvothermal method: The hydro/solvothermal approach is one of the most extensive and adaptable methods for producing nanoparticles with desired morphology and controlled size. In a conventional procedure, reactants (metal salts) are dissolved in water, an organic solvent, or a combination of both. The solution is then placed in an autoclave made of Teflon-coated stainless steel, heated to a specific temperature, and held for a predetermined time. By adjusting the reaction conditions, we can precisely regulate the resultant materials' size, shape, and crystallinity. This technique is often used to create zeolites, nanowires, and nanoparticles.

Electrochemical deposition: This method deposits material onto an electrode surface using an electrochemical cell from a solution containing metal ions or other precursor species. The precursor species are reduced or oxidised when a voltage or current is applied, which causes a thin film or coating to develop on the electrode.

Electrochemical deposition is often utilised to fabricate thin films, coatings, and patterned structures.

Precipitation: One of the most used preparation techniques is precipitation, often utilised to make bulk materials with precise control over particle size and content. Precipitation is the creation of solid particles from a solution by adding a reactant that creates insoluble compounds. Filtration or centrifugation are two methods for separating the final solid particles.

2.3 Material Characterization Techniques

The characterisation techniques used in this study are described in the following section. The following section provides a quick overview of each method's fundamentals. Here is a list of the main techniques used which is shown in Fig. 2.1.

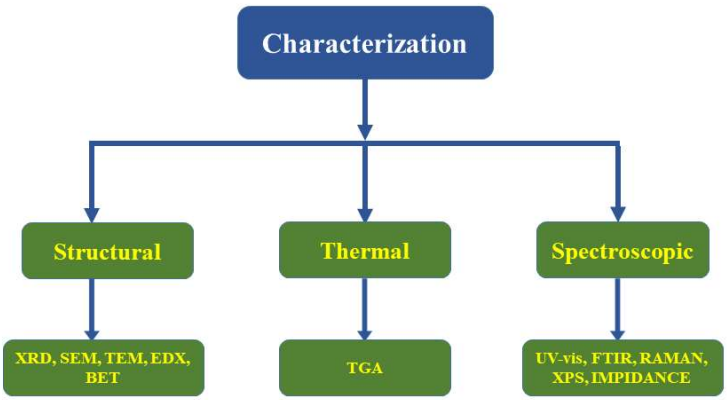

Figure 2.1 Characterization techniques used

2.3.1 X-Ray Diffraction (XRD)

The most potent, popular, and flexible method is X-ray diffraction (XRD), used to investigate solid samples qualitatively and quantitatively at the atomic and molecular level. It measures the structural properties, including grain size, crystallite size, phase composition, preferred orientation, defect structure, strain state, and epitaxy of these phases present in the compound. The structure of a material, allotropic transformation,

transition to different phases, material purity, lattice parameters, and the presence of external atoms in the crystal lattice of an active component are also all determined by this method. [14] Materials having various element compositions can be effectively identified with XRD. However, because of the vast diffracted intensities of the sizeable atomic number elements compared to those with lower atomic numbers, sizeable atomic number elements are susceptible to X-rays. It foretells the quantitative phase analysis and qualitative microstructural and structural analysis.

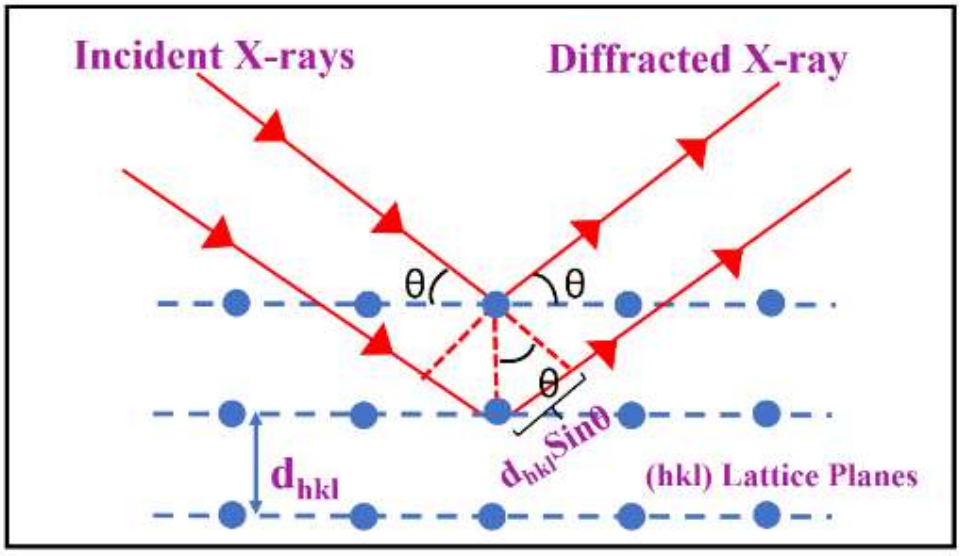

Figure 2.2 Schematic diagram of the incident and diffracted X-rays from the crystal lattice (Adapted from [16])

The fundamental idea behind X-ray crystallography is diffraction, a phenomenon where X-rays are produced from an X-ray tube and filtered into a monochromatic single wavelength frequency. These reflected rays were counted throughout the angle and diffraction ranges that vary by the relation

$$n\lambda = 2d \sin\theta \qquad (2.1)$$

where, d is the spacing between diffracting planes, θ is the incident angle, n is an integer, and λ is the beam's wavelength. [15] Bragg's law is illustrated in Fig. 2.2. The symmetry of the material's structure affects the diffraction peaks.

The diffraction patterns of the prepared samples were recorded on an X-Ray diffractometer instrument (Rigaku miniflex) using Ni-filtered Cu Kα radiation as the X-ray source having wavelength 1.5406 Å. The applied voltage was 30 kV and 15 mA. The X-ray diffraction pattern was measured within the 10°- 80° 2θ range with a slow-scanning rate having a step size of 0.02°.

The Rietveld refinement of the powder XRD patterns was carried out by using FullProf Suite. Xpert High Score (PANanylytical) which is a frequently used refinement technique for powder X-ray diffraction (XRD) based on the method proposed by Hugo Rietveld in the 1960s. [17] The Rietveld approach involves fitting a calculated profile (including all the structural and instrumental parameters) to the experimental data. It employs the non-linear least-squares technique and requires a reasonable approximation of many free parameters in the initial stage, including peak shape, unit cell dimensions, and all the atomic coordinates in the crystal structure. Other parameters can be refined reasonably by guessing. In this way, refinement of the crystal structure of a powder material from the PXRD data can be performed. The successful outcome of the refinement method is directly related to the data quality of the model (includes initial approximation) and the user's experience.

2.3.2 Scanning Electron Microscope (SEM)

The particle size, surface shape and chemical composition of the sulfide and oxide materials were determined by SEM analysis with NOVA Nano SEM 450 equipped with EDAX - Ametek detector. Scanning electron microscopy can provide detailed

resolution images of the sample by refocusing an electron beam through the sample's surface and collecting secondary or backscattered electron signals. An energy-dispersive X-ray analyser (EDX or EDAX) also acquires element detection and quantitative compositional information. SEM offers images with a magnification of up to X50,000, making it possible to observe features far smaller than the optical microscope's field of view or sub-micron-scale features. The elemental composition of a samples can be determined using an X-ray technique called EDX. Fig. 2.3 shows a schematic image the of HR-SEM. [19]

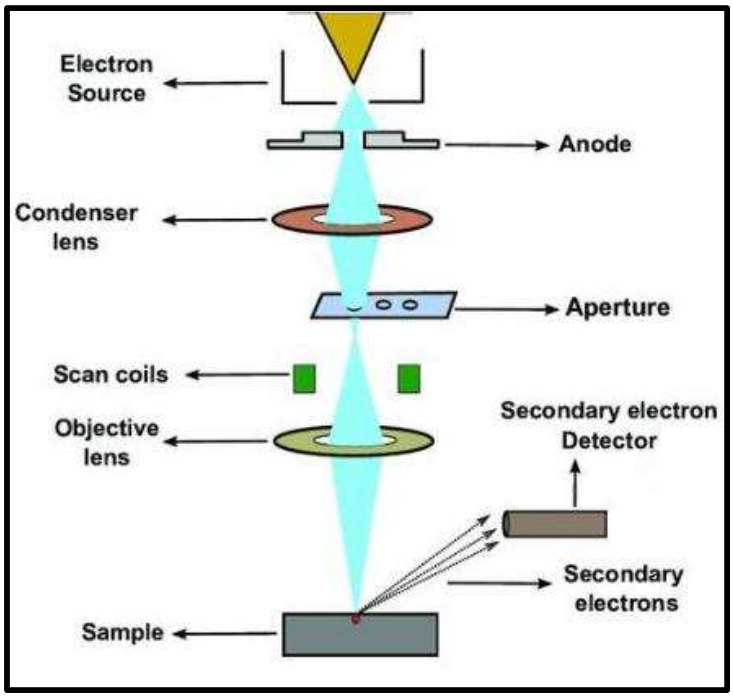

Figure 2.3 Schematic diagram of SEM operating (Adapted from [18])

2.3.3 Transmission Electron Microscopy (TEM)

The powerful tool and widely utilised transmission electron microscopy (TEM) method is used to characterise materials and study their particle size distribution. By interacting a high-intensity electron beam with the atoms in the material, the electrons produce

pictures that can be utilised to identify aspects like the crystal structure, its dislocations, and the limits and shapes of the grain.

Transmission electron microscopes, which use de Broglie wavelengths that are a fraction of an angstrom smaller than those used in light microscopes, offer far greater resolution. Due to this equipment characteristic, capturing even single atoms, which are 1,000 times smaller than an item under a light microscope, is feasible. The transmission electron microscope (FEI Tecnai G^2 20 TWIN, USA) used a LaB6 filament and an accelerating voltage of 200 kV to produce bright-field TEM micrographs and selected area diffraction patterns (SAED). Samples were diffused in 20 ml of anhydrous ethanol and sonicated for 30 minutes before a drop is placed on a holey-carbon-coated copper grid (Pelco International, USA) for TEM imaging. HRTEM micrographs were recorded and analyzed with Gatan Microscopy Suite (Digital Micrograph) and ImageJ software. [20, 21]

Lattice images and electron diffraction patterns are two types of data that provide a window into crystallographic data in TEM. After entering the sample, most electrons interact with the specimen by being elastically scattered by the atoms' nuclei. The atoms' nuclei in the specimen cause certain electrons to scatter inelastically (Fig. 2.4). The interaction of electrons with the sample is much greater than that of X-ray or neutron diffraction, and many scattering events are anticipated. An incoherent particle model may explain the interaction of the electrons with the material for thick specimens at lower resolutions.

The electrons passing through the sample close to the nucleus are slightly accelerated, resulting in a slight local decrease in their wavelength and a minor electron phase shift. Therefore, the electron phase receives information on the specimen structure. Only the

elastically scattered electron is significant for the creation of high-resolution pictures. The background of the image is mainly made up of inelastically dispersed electrons. The inelastically scattered electrons also produce Kikuchi lines in the electron diffraction pattern, which is helpful for the crystal's accurate crystallographic alignment in the specimen. [20]

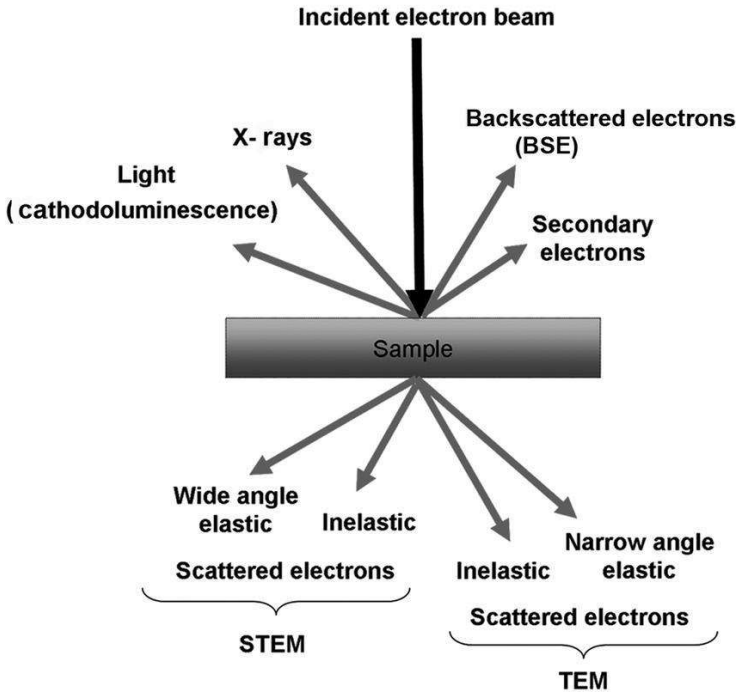

Figure 2.4 Schematic diagram of TEM showing interaction of electrons with sample (Adapted from [20])

2.3.4 Energy Dispersive X-Ray Spectroscopy (EDS)

Energy dispersive X-ray spectroscopy, also known as EDS, EDX, EDXS, or XEDS, is a non-destructive technique used for determining the elemental composition of materials. It is sometimes called energy dispersive X-ray analysis, EDAX. This is often attached to structural analysis methods like SEM and TEM, which utilise a high-energy electron beam and electrons expelled from an atomic orbital's inner shell to identify the specimen of interest. The resulting internal shell vacancy is filled by electrons in the

shell close to the vacant shell; these transitions generate X-rays. As a result, using the energy of the released X-rays, it is possible to analyse the information relating to the elements within the samples. Sometimes X-ray mapping may not show the correct

distribution of elements that are not of interest because the characteristics of X-rays of elements of interest are close to those not desired. It occurs when the energy difference between the wanted and unwanted components equals the spectrometer's resolution. This technique, also known as quantitative sample mapping, statistically assesses the spots on the sample while scanning the electron beam. In this thesis, we investigated the composition's electron mapping using EDAX in combination with SEM. [22]

2.3.5 BET (Brunner-Emmett-Teller Theory) Surface Area Measurement

Pore size distribution and specific surface area of the sample were analyzed using BET (BELCAT-II, MicrotracBEL Corp.) which uses the physical adsorption of a gas (nitrogen gas) on a solid's surface to determine the surface area of that solid. The determined surface areas will further assist in understanding moisture retention, catalytic activity, and shelf life. Van der Waals force between the adsorbent and the adsorbate is involved in physical adsorption. Gases will desorb after adsorption. Therefore, the quantity of adsorption of a gas on the adsorbent will determine the required specific surface area of the sample. The BET process is often carried out in an isothermal environment using liquid nitrogen to maintain a constant temperature. On the other hand, the adsorbate gas's pressure or concentration continued rising. As a result, a graph has been drawn connecting the volume adsorbed onto the sample with the relative pressure of the gas. [23, 24]

BET is carried out in three steps:

1. The reference cell was standardised.

2. Heating the sample at a specific temperature as a pre-treatment.

3. Under isothermal circumstances, adsorbate is adsorbed to the adsorbent.

2.3.6 TGA-DSC

Thermogravimetric analysis (TGA) and differential scanning calorimetric (DSC) analysis are two analytical techniques for thermal study. This technique determines the mass transformation as a function of temperature while maintaining a uniform heating rate or duration and a constant mass loss. The sample's stable temperature, or the temperature at which it can be calcined to produce, was determined using TGA analysis. The thermal stability of sulfide samples was investigated by thermal gravimetric analysis (TGA) and simultaneous thermal analyzer (STA) 6000 (PerkinElmer Pvt. Ltd) instrument with a varying temperature range from 50 to 700 °C using a heating ramp rate at 10 °C min^{-1}.

In addition, the combined TGA/DSC analysis provides insight into the reaction pathway for the prepared mixture of raw materials and several transition points, including melting point, crystalline temperature, glass transition temperature, etc. In this thesis, various materials were subjected to TGA and DSC measurements at temperatures ranging from 30 to 700 °C in an environment of nitrogen gas. [25]

2.3.7 UV-Visible Spectrophotometer

The UV-Visible spectra of the sulfide samples was recorded in the 200–800 nm range using an Agilent Cary 60 UV-visible spectrophotometer. This method helps determine substances' band gap and absorption characteristics in the visible and adjacent (near-ultraviolet and near-infrared) ranges. A material gets excited by absorbing light in the UV-visible region and produces absorption spectra which is then used to determine the bandgap of the semiconductors. The absorbance is measured

concerning a reference, and a graph of absorbance *vs* wavelength is plotted. Fig.2.5 displays the schematic illustration of the UV-visible spectrophotometer. The difference between the absorbed light intensities of the sample and the reference cell is measured in this investigation to determine the sample's absorption characteristics. [26]

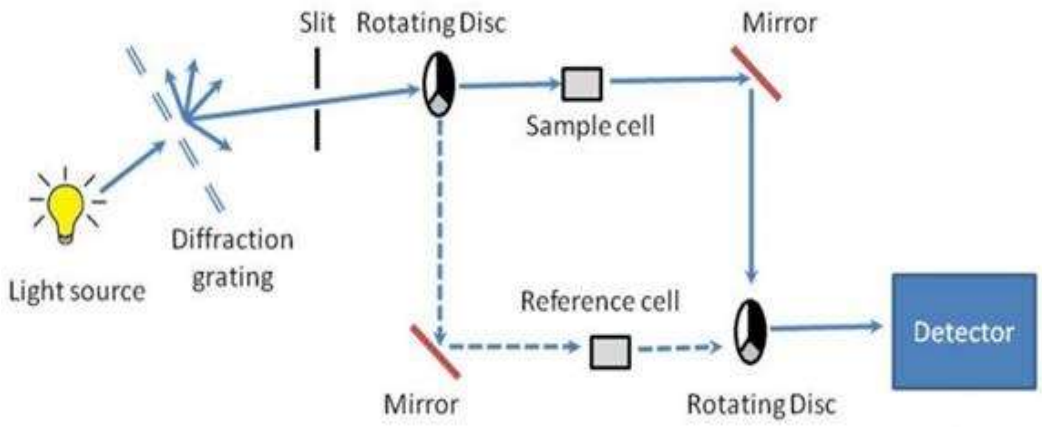

Figure 2.5 Schematic diagram of UV-Visible spectrometer (Adapted from [27])

2.3.8 Fourier Transform Infrared (FTIR) Spectroscopy

At specific quantized energy levels, the atoms present in a molecule show vibration and rotation in various ways. A molecule's infrared spectrum results from its atoms' vibrations and rotations, affecting its permanent dipole moment. The infrared absorption spectrum generated by FTIR may be used to determine the existence of particular functional groups in a molecule and covalent bonding information. The FTIR spectrum of distinct molecular fingerprints can screen and scan samples for many different components. A light source, monochromatic slit, beam splitter, detector, and analogue recorder make up an FTIR spectrometer. The FTIR spectra of sulfide materials was measured with Thermo Scientific Nicolet iS5 FTIR spectrometer and data were recorded within 400-4000 cm^{-1} using KBr pellet. [28]

2.3.9 Raman Spectroscopy

Raman spectroscopy is an effective and non-destructive tool to characterize materials using the inelastic scatting of monochromatic light. Raman spectroscopy has been extensively applied to identify the defect and layer number in 2D materials. The electromagnetic field (EMF) and materials/molecules interact, causing inelastic scattering, which forms the basis of Raman spectroscopy. The analysing molecule interacts with the incoming EMF or photons, and a dipole moment is induced that is directly correlated with the polarizability of the molecule. According to Raman's study, inelastic scattering occurs when the incoming and scattered photon wavelengths vary; the higher wavelength is the Stokes line, and the lower is the anti-Stokes line. The Raman signal's intensity is very weak compared to the incident laser, i.e., single inelastic scattering out of one million scatterings. The shorter wavelength laser produces a more robust signal because it has more considerable Raman scattering (inelastic scattering) cross-sections. The sulfide samples' Raman spectra were recorded using a Renishaw Raman microscope with a 633 nm laser showed the prepared samples' chemical characteristics. [29, 30]

2.3.10 X-Ray Photoelectron Spectroscopy (XPS)

X-ray photoelectron spectroscopy (XPS) is a technique providing surface compositional information, bond type, valence and electronic states of the elements. The sample is subjected to an intense beam of X-rays with a specific energy range to conduct XPS. These X-rays are absorbed by the electrons associated with the sample's atoms, and some of the electrons are subsequently ejected from the sample's surface; the electrons are called photoelectrons. Low-energy photoelectrons have an escape depth of around 10 nm, close to the sample's surface. The energy of the ejected electrons is measured, giving information on the atomic species and the types of bonds

present in the sample. The spectra are produced by illuminating a solid surface with an X-ray beam and measuring the kinetic energy of the electrons released from the top 1 to 10 nm of the material under investigation. Thermo Fisher Scientific's K-Alpha spectrometer equipped with an aluminium (Al Kα radiation) monochromator source operating at 15 kV and 20 mA was used to conduct the XPS of samples. [31]

2.3.11 Electrochemical Measurements

The electrochemical performance of the assembled electrode prepared for the supercapacitor/pseudocapacitor is evaluated using electrochemical measurements. Cyclic voltammetry (CV), galvanostatic charge-discharge (GCD), and electrochemical impedance spectroscopy (EIS) are three principal techniques that measure electrochemical performance.

2.3.11.1 Cyclic Voltammetry (CV)

Cyclic voltammetry (CV) is a unique, significant, and extensively used electrochemical technique in analytical chemistry which measures the current that develops in an electrochemical cell for a better understanding of electrode reaction mechanism and the characteristics of charge transfer reactions between electrolyte ions and electrons from the electrode surface. Consequently, cyclic voltammetry is a powerful method for studying the redox reaction, which is crucial to the supercapacitor's/pseudocapacitor's charge storage technique. It is widely used as it can provide the basic information of a capacitive electrochemical cell, such as capacitance, voltage window and cycle life. To measure the current, cyclic voltammetry involves changing the applied voltage at a working electrode in both forward and backward directions at various scan speeds.

A three-electrode system (Fig. 2.6) is the cell's basic configuration to comprehend the sample's electrochemical behaviour. A working electrode (WE), counter electrode (CE)

and reference electrode (RE) constitute a three-electrode setup. Potentiostat will control the potential between WE and CE while it measures the potential difference between WE and RE. The device controls the current flowing between WE and CE like a galvanostat. The potential difference of WE concerning RE and the current flowing between the CE and WE are continuously analyzed by AfterMath software (Pine research instrument WaveDriver-200). [32]

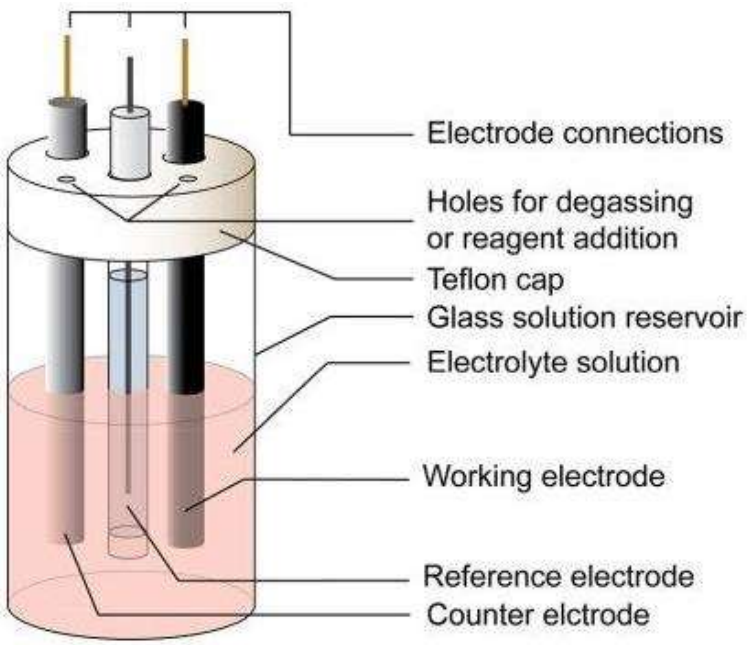

Figure 2.6 Three electrodes setup used in electrochemical measurement (Adapted from [33])

The electrode over which the interested reaction occurs is the working electrode. A current collector may be made of glassy carbon, graphite sheet, carbon sheet, or carbon paper over which active material/working electrode has been coated. The counter electrode displays inert behaviour, typically excluding the electrochemical process, such as platinum, gold, graphite, and glassy carbon. These counter electrodes have closed the electrochemical cell's current circuit. Ag/AgCl, and saturated calomel electrode (SCE) are reference electrodes with well-known electrode potentials.

2.3.11.2 Galvanostatic Charge-Discharge (GCD)

Similar to the CV technique, the GCD technique measures the electrochemical performance of supercapacitor electrodes through the charge and discharge cycle in a controlled current condition. In the GCD measurement, the current is constant/controlled, and voltage is measured when the current pulse is applied to the working electrode. About the time function, the resultant voltage is recorded against the reference electrode. When a constant current is applied, measured potential changes abruptly; due to internal resistance, it changes gradually due to over-potential developed across the electrode as the concentration of the reactant is exhausted at the electrode surface. [34] Using GCD technique the parameters such as specific capacitance, resistance and cyclability of electrode material can be calculated. From the GCD curve, the specific capacitance, C_{sc}, of the electrode can be calculated by the equation given below:

$$C_{sc} = \frac{i\Delta t}{m\Delta V} \qquad (2.2)$$

Where i is the discharge current in A, Δt is the discharge time in s, m is the mass over electrode of active material in g, and ΔV is the potential change during discharge in V.

2.3.11.3 Electrochemical Impedance Spectroscopy (EIS)

EIS measurement was conducted to comprehend the cyclic capacity or capacitance fading in pseudocapacitance. A graph known as a "Nyquist plot" (Fig. 2.7) has been plotted with EIS measurement data by placing imaginary impedance ($Z_{imaginary}$) at the y-axis and real impedance (Z_{real}) at the x-axis. A semicircle is often seen in the high-frequency and low-frequency bands of an EIS measurement. The EIS measurements were studied to evaluate the electrode kinetics and interface resistance at an open circuit potential from 100 kHz to 0.1 Hz. The impedance distributions across electric series

resistance (R_s), charge transfer resistance (R_{ct}), and Warburg impedance (R_w) are primarily responsible for the specific impedance contribution.

The real axis intercept in the EIS spectra at higher frequencies shows negligible internal resistance. The tiny semicircle in the high-frequency area also demonstrates the rapid charge transfer between the electrode and electrolyte. The straight line in the low-frequency area is relatively near the -Z"(Ω) axis from the horizontal line, reflecting the characteristic of pseudo-capacitance behaviour. Lower frequency data indicate the Warburg diffusion resistance. This also represents fast ion diffusion in the porous structure. [34, 35]

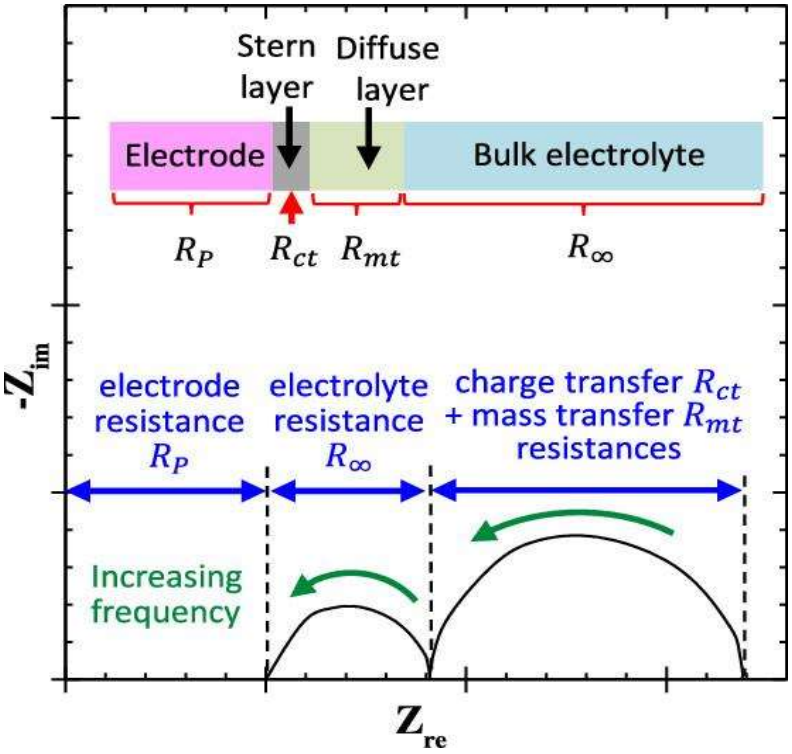

Figure 2.7 Typical Nyquist plot for electrode (Adapted from [35])

2.4 Electrode Fabrication

Before combining, the powder forms of the active ingredients-active materials (sulfides and oxide materials), activated carbon, and polyvinylidene fluoride (PVDF)

(binder) are pre-weighed. The three components are thoroughly mixed and grounded in a mortar, and then a tiny quantity of N-methyl pyrrolidinone (NMP) or tetra hydro furan (THF) solvent and was added to create a slurry. Using a micropipette, the slurry was evenly placed on Toray carbon paper used for pseudocapacitor/supercapacitor application having (coating area: 1 cm^2, total mass loading: ~1 mg). The newly constructed electrodes are immediately placed in an electric oven and vacuum-dried at 90 °C overnight. The assembled electrode for the investigation is shown in Fig. 2.8.

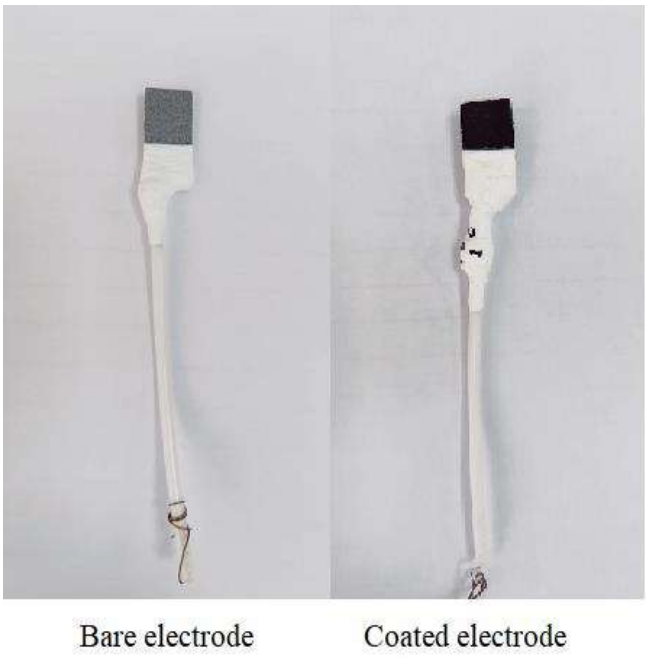

Figure 2.8 Assembled electrode picture for electrochemical measurement

2.5 Cell Assembly

A working electrode (material-coated Toray carbon paper) facing a counter electrode (platinum wire) and reference electrode (SCE or Hg/HgO or Ag/AgCl), which was placed close to the working electrode, were assembled for the pseudocapacitor/supercapacitor performance test. 2 M KOH and 0.5 M Na_2SO_4 were used as the electrolytes. The three-electrode cell was left for ~1-2 hours

before electrochemical testing so that the electrolyte solution could penetrate the working electrode through pores.

2.6 References

1. Abid, N., et al., *Synthesis of nanomaterials using various top-down and bottom-up approaches, influencing factors, advantages, and disadvantages: A review.* Advances in Colloid and Interface Science, 2022. **300**: p. 102597.
2. Ma, T., et al., *Nickel-cobalt-molybdenum sulfides with adjustable morphology via coprecipitation and hydrothermal conversion as high-performance electrodes for asymmetric supercapacitors.* Journal of Alloys and Compounds, 2020. **838**: p. 155631.
3. Nwodo, I.C., et al., *Synthesis and characterization of co-precipitated nickel phosphate [Ni3 (PO4) 2] nanoparticles prepared at varying precursor concentrations.* Journal of the Indian Chemical Society, 2023. **100**(7): p. 101026.
4. Islam, S., et al., *Recent Advancements in Electrochemical Deposition of Metal-Based Electrode Materials for Electrochemical Supercapacitors.* The Chemical Record, 2022. **22**(7): p. e202200013.
5. Chen, W., C. Xia, and H.N. Alshareef, *One-step electrodeposited nickel cobalt sulfide nanosheet arrays for high-performance asymmetric supercapacitors.* ACS nano, 2014. **8**(9): p. 9531-9541.
6. Pore, O., et al., *Review on recent progress in hydrothermally synthesized MCo2O4/rGO composite for energy storage devices.* Chemical Engineering Journal, 2021. **426**: p. 131544.
7. Jin, J., et al., *Hydrothermal synthesis of NiO/NiCo 2 O 4 nanomaterials for applications in electrochemical energy storage.* Journal of Materials Science: Materials in Electronics, 2022: p. 1-13.

8. Li, J., et al., *Nanomaterials Derived from a Template Method for Supercapacitor Applications.* ChemistrySelect, 2023. **8**(24): p. e202204487.

9. Yan, B., et al., *Facile self-template synthesis of a nitrogen-rich nanoporous carbon wire and its application for energy storage devices.* ACS Applied Energy Materials, 2021. **4**(12): p. 13735-13747.

10. Grover, V., B.P. Mandal, and A. Tyagi, *Solid State Synthesis of Materials.* Handbook on Synthesis Strategies for Advanced Materials: Volume-I: Techniques and Fundamentals, 2021: p. 1-49.

11. Smida, Y.B., et al., *Synthesis methods in solid-state chemistry*, in *Synthesis Methods and Crystallization*. 2020, IntechOpen.

12. Ushio, M. and Y. Sumiyoshi, *Synthesis of ZnO single crystals by the flux method.* Journal of materials science, 1993. **28**(1): p. 218-224.

13. Hsu, J.W., *Solution Synthesis, Processing, and Applications of Semiconducting Nanomaterials*. 2019, MDPI. p. 1442.

14. Drits, V., J. Środoń, and D. Eberl, *XRD measurement of mean crystallite thickness of illite and illite/smectite: Reappraisal of the Kubler index and the Scherrer equation.* Clays and clay minerals, 1997. **45**: p. 461-475.

15. Cullity, B.D., *Elements of X-ray Diffraction*. 1956: Addison-Wesley Publishing.

16. Guo, J., et al. *Numerical Analysis of Structural Color for Photonic Crystal Hydrogel*. in *Photonics*. 2023. MDPI.

17. Rietveld, H.M., *A profile refinement method for nuclear and magnetic structures.* Journal of applied Crystallography, 1969. **2**(2): p. 65-71.

18. Marturi, N., *Vision et asservissement visuel pour la nanomanipulation et la nanocarectérisation sous microscope électrique à balayage*. 2013, Université de Franche-Comté.

19. Scimeca, M., et al., *Energy Dispersive X-ray (EDX) microanalysis: A powerful tool in biomedical research and diagnosis.* European journal of histochemistry: EJH, 2018. **62**(1).

20. Williams, D.B. and C.B. Carter, *Transmission Electron Microscopy: Spectrometry. IV*. 1996: Plenum Press New York.

21. Amelinckx, S., et al., *Electron microscopy: principles and fundamentals*. 2008: John Wiley & Sons.

22. Hodoroaba, V.-D., *Energy-dispersive X-ray spectroscopy (EDS)*, in *Characterization of Nanoparticles*. 2020, Elsevier. p. 397-417.

23. Naderi, M., *Surface area: brunauer–emmett–teller (BET)*, in *Progress in filtration and separation*. 2015, Elsevier. p. 585-608.

24. Bardestani, R., G.S. Patience, and S. Kaliaguine, *Experimental methods in chemical engineering: specific surface area and pore size distribution measurements—BET, BJH, and DFT.* The Canadian Journal of Chemical Engineering, 2019. **97**(11): p. 2781-2791.

25. Morgan, D., *ME Brown. Introduction to Thermal Analysis: Techniques and Applications. London and New York (Chapman and Hall), 1988. viii+ 211 pp., 113 figs. Price£ 17.50.* Mineralogical Magazine, 1989. **53**(373): p. 662-662.

26. Ojeda, C.B. and F.S. Rojas, *Recent applications in derivative ultraviolet/visible absorption spectrophotometry: 2009–2011: A review.* Microchemical Journal, 2013. **106**: p. 1-16.

27. Mohanta, D., *A DETAILED STUDY ON OPTICAL AND PHYSICAL PROPERTIES OF RICE AND ITS BY-PRODUCTS*. 2017, Tezpur University.

28. Griffits, P. and J.A. de Haseth, *Fourier transform infrared spectrometry.* Chemical Analysis, 2007. **53**.

29. Schlücker, S., *Surface-Enhanced raman spectroscopy: Concepts and chemical applications.* Angewandte Chemie International Edition, 2014. **53**(19): p. 4756-4795.

30. Ferraro, J.R., *Introductory raman spectroscopy*. 2003: Elsevier.

31. Van der Heide, P., *X-ray photoelectron spectroscopy: an introduction to principles and practices*. 2011: John Wiley & Sons.

32. Elgrishi, N., et al., *A practical beginner's guide to cyclic voltammetry.* Journal of chemical education, 2018. **95**(2): p. 197-206.

33. Bzainia, A., *Preparation and Ionic Transport Properties of Conductive Polymers for Dye-Sensitized Solar Cells*. 2019, Instituto Politecnico de Braganca (Portugal).

34. Bard, A.J. and L.R. Faulkner, *Fundamentals and applications: electrochemical methods.* Electrochem. Methods, 2001. **2**(482): p. 580-632.

35. Mei, B.-A., et al., *Physical interpretations of electrochemical impedance spectroscopy of redox active electrodes for electrical energy storage.* The Journal of Physical Chemistry C, 2018. **122**(43): p. 24499-24511.